# Ceres:

# The evolution of the interior and surface

Joshua Gaal

November 22, 2016

Advisor: Dr. Nicholas Schmerr

GEOL394

#### **Abstract**

Ceres is the largest object in the asteroid belt, comprising one-third the mass of the asteroid belt, with a density of 2150 kg/m<sup>3</sup> (Neveu and Desch 2016). The internal structure of Ceres is uncertain, with multiple models proposed. The Dawn mission was designed and launched by NASA to rendezvous with and orbit Vesta and Ceres in order to characterize them. The rendezvous of Dawn with Ceres in 2015 marked the beginning of its mission of characterizing the internal structure. density, shape, size and mass of Ceres while also returning data about its surface features and magnetism. While Ceres was once thought to have a surface rich in ice, spectroscopic data from Dawn shows a lack of water ice while demonstrating surficial clays (McSween et al. 2016). Given current information, there are several models for the internal structure of Ceres that are acceptable, from an undifferentiated Ceres to a differentiated Ceres with an iron core. The moment of inertia can be used to constrain possible internal structures, due to the relationship between the distribution of mass within an object and the density of an object. The moment of inertia of Ceres can be calculated based on changes in the gravity field due to differences in mass. Here I show a density stratification model to plot the relationship between interior density, exterior density, and interior radius, as constrained by the moment of inertia. Using a three-phase mixing model provides a constraint on the range of compositions for a given exterior density. My results suggest a stratified Ceres with an exterior density between 1400 kg/m<sup>3</sup> and 1800 kg/m<sup>3</sup> and an interior density between 2649 kg/m<sup>3</sup> and 3259 kg/m<sup>3</sup>. The range of exterior densities suggests the exterior contains 20% to 30% pore space, with the remaining material being composed of 30% to 60% water ice and 40% to 70% clay. The range of interior densities suggests an interior composed of rock with a silicate composition or a basaltic composition. The clay on the surface of the Ceres suggests that liquid water may have been present. The clay may have formed in situ through water-rock interaction, however, the surface conditions of Ceres do not allow for the presence of liquid water. Raising the pressure on the surface would allow liquid water to form, and this pressure increase can come from an ice shell, which could be lost over time due to processes such as interaction with solar wind and impacts. The rates of loss of hydrogen from Venus and Mars due to solar wind were used to calculate comparative rates of loss for Ceres, which was used to calculate the amount of ice that could have been stripped form the surface of Ceres throughout its history. Using Venus, the thickness of a uniform ice shell around the surface of Ceres could be between 1.3 and 20.2 m, and using Mars, the thickness of a uniform ice shell could be between 6.1 and 192.1 m. The Mars based range of values is thick enough to raise the pressure to support liquid water, supporting the hypothesis that surficial liquid water was possible in the geologic history of Ceres. The lower bound of the Venus based range does not support this hypothesis.

## **Introduction and Background**

Asteroids and their compositions are of both scientific and economic interest. Asteroids are the remnants from the formation of the solar system, and can provide knowledge about the composition of rocky bodies as they formed (Nelson et al. 1993). Asteroids contain materials that could have a host of industrial uses: water, which could be used for life support or propulsion; metals, such as iron or nickel, which can be used in construction; metals, such as gold, platinum, and copper, which have electrical uses (Ross 2001). Although the composition of the surface of an asteroid can be examined by telescopic reflectance spectroscopy, there are currently few constraints for the interiors of specific asteroids. The only evidence for the compositions of asteroid interiors is the collection of meteorites on Earth; these meteorites provide knowledge on the interiors of asteroids as a whole, but cannot always be used to determine their asteroid of origin, because the interior is not subjected to the same processes as the surface (Nelson et al. 1993).

NASA launched the Dawn mission in 2007 to rendezvous and orbit Vesta and Ceres and characterize their internal structure, density, shape, size, and mass and returning data on surface morphology, cratering, and magnetism. The instruments on the Dawn spacecraft include: a magnetometer boom, cameras, a mapping spectrometer, a laser altimeter, star trackers, and a gamma ray/neutron spectrometer. The data collected during this mission will aid in determining thermal history, size of cores, and the role of water in asteroid evolution. <sup>1</sup> The rendezvous of Dawn with Ceres in 2015 has already presented information for researchers. Analysis of data gathered from a low altitude mapping orbit shows that the regolith of Ceres is rich in hydrogen relative to Vesta, has a carbonaceous chondrite like composition, and likely contains water ice near the surface (Prettyman et al. 2016). The approach to a high-altitude mapping orbit was able to provide data used to determine the shape and gravity field of Ceres (Park et al. 2016).

Ceres is the largest object in the asteroid belt, and was discovered in 1801 by Giuseppe Piazzi while attempting to find the planet predicted by the Titus-Bode law (McCord and Sotin 2005). At  $9.4 \times 10^{20}$  kg, Ceres comprises one-third of the mass of the asteroid belt, and is roughly spherical with the shape profile of  $482 \times 480 \times 446$  km. From these figures, Ceres is calculated to have a bulk density of approximately  $2150 \text{ kg/m}^3$  (Neveu and Desch 2016). This bulk density is about 20% less than a previous estimate of about  $2700 \text{ kg/m}^3$ , a value obtained 30 years ago using the occultation method (Millis et al. 1987). This density is much less than those of silicate bodies, such as Vesta or the Moon, suggesting a mixture of lighter materials or increased porosity (Park et al. 2016).

There are a variety of compositions and internal structures that have been proposed to explain the accepted density of  $2150 \text{ kg/m}^3$ . Surface spectroscopy is an important tool for determining the surface composition. A  $3.05 \mu m$  band was initially interpreted as water ice in the 1980s, but it was later determined that water ice is not very stable on Ceres (Rivkin et al. 2006). In the 1990s, clays were suggested as a better fit, but no such materials had been seen in meteorites (Rivkin

\_

<sup>&</sup>lt;sup>1</sup> http://nssdc.gsfc.nasa.gov/planetary/planets/asteroidpage.html

et al. 2006). The data returned from the Dawn Visible and near-InfraRed spectrometer support a clay-rich surface of ammoniated phyllosilicates along with other hydrous minerals, opaques, and carbonates (Prettyman et al. 2016). Additionally, no spectral feature of water ice is present on Ceres, but the bulk density has caused suggestions of water content between 17 wt. % and 35 wt. % that takes the form of water of hydration, ice, or water (McSween et al. 2016, McCord and Sotin 2005).

Multiple models have been proposed for the interior of Ceres, ranging from undifferentiated (McCord and Sotin 2005, Zolotov 2009) to four-layered differentiation (Castillo-Rogez and McCord 2010). McCord and Sotin (2005) present several evolution scenarios, ranging from no differentiation to fully differentiated models with an iron core (**Figure 1**). Their undifferentiated model is composed of 74% by mass silicates and 26% by mass water ice. This model assumes rapid accretion of smaller bodies, and internal temperatures are high enough for liquid water in the interior. They provide three differentiated models, with two of models being very similar, with a difference primarily based on the presence of some material acting as an anti-freeze, such as ammonia or salt. The first of these two models has three layers: a silicate core, a convective ice layer, and a thin conductive ice lid. The second of these models is modified by the presence of materials that act as anti-freeze, such as ammonia or salts, that result in a four-layered structure: a silicate core, a liquid water ocean, a convective ice layer, and a thin conductive ice lid. The silicate cores of these models have a variable thickness, based on their assumed composition. McCord and Sotin (2005) use the end members of a highdensity core similar to Vesta and a low-density serpentine core, which affect core size. Their final model makes the assumption that already differentiated bodies with iron cores accreted, leading to an iron-rich inner core.

Unlike McCord and Sotin's (2005) undifferentiated, three-, or four-layer models, Neveu and Desch (2016) presented a two-layer model consistent with pre-Dawn and preliminary Dawn data, assuming Ceres accreted ice and small ( $\mu$ m- and mm-sized) rock particles, yielding a chondrule-based core and a mantle of mixed ice and fines. Zolotov (2009) argues that a lightly differentiated or undifferentiated Ceres cannot be excluded, with observations from different sources yielding different interpretations on differentiation. Physical characteristics do not support an interior water layer, with impact structures not revealing signs of ice, and surface roughness may imply a thick rocky layer over a water ice mantle, though this would be gravitationally unstable (Zolotov 2009). Zolotov (2009) argues that with compositionally homogenous models, an abrupt collapse of porosity accounts for the parameters that characterize a stratified body.

Furthermore, any water ice undergoing the transition to gas on the surface of a body can be stripped through thermal and non-thermal processes, such as Jean's Escape and interaction with solar wind. Water vapor and water ice can also be ejected from around a body through impacts. Ceres is susceptible to this form of loss due to the low surface gravity, allowing the material to be ejected without being pulled back to the surface. Solar wind is capable of stripping atoms from bodies if the atoms are ionized, which can occur through charge exchange with protons or processes such as photoionization (Chalov S. 2006). The ions can then be picked up

by the charged solar wind (Lammer et al. 2006). The ejection of material from the surface of Ceres is supported by the lack of missing craters on Ceres (Castillo-Rogez et al. 2016). Estimations of the number of large impact craters that should be present on Ceres range from 6 to 15 craters larger than 400 km, yet the surface of Ceres is devoid of impact craters larger than 280 km (Marchi et al. 2016). Castillo-Rogez et al. (2016) suggest the current surface of Ceres is the base of an original shell and may explain some of the surficial clays through the slow release of heat.

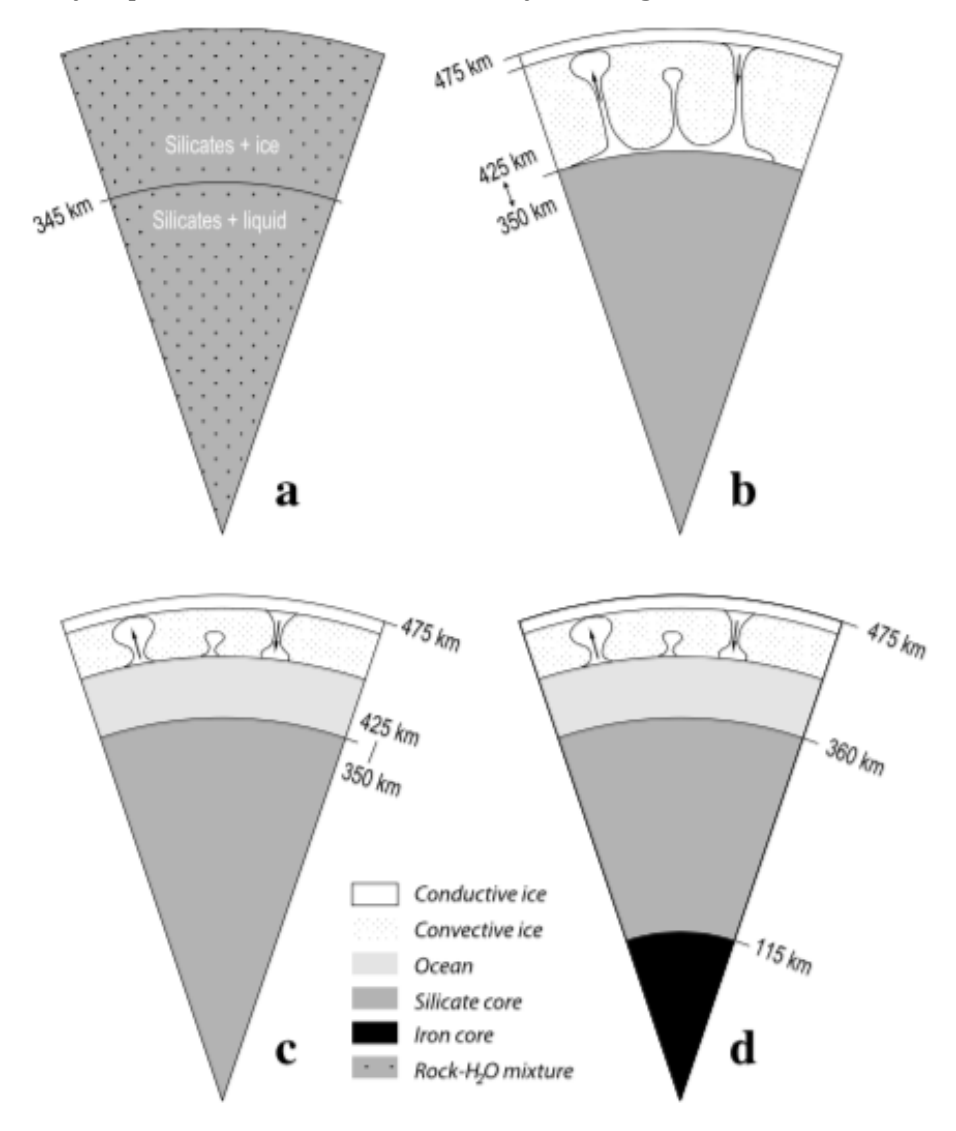


**Figure 1.** McCord and Sotin's (2005) internal structures based on different scenarios. a) Undifferentiated Ceres composed of a water-silicate mix. b) Differentiated Ceres with Vesta-like high-density core (350 km core radius) or low-density serpentine (425 km core radius). c) Same as b), but with anti-freeze materials, such as ammonia, maintain a liquid layer. d) Differentiated Ceres with iron core.

### **Objectives of Research and Broader Implications**

I tested the hypothesis that Ceres was differentiated into a body that has segregated into an exterior and interior of separate and distinct compositions, with volatiles and clay in the exterior and rock or metals in the interior. I tested this by modeling the possible internal models of Ceres using known physical parameters such as moment of inertia obtained by the Dawn mission, and by matching this to a range of exterior compositions for a given exterior density.

I tested the hypothesis that liquid water could be sustained on the surface of Ceres in the past by a layer of subsequently removed ice. I tested this by calculating the loss of hydrogen from the surface of Ceres due to interactions of this layer with solar wind over time based on the rate of loss of hydrogen from Venus and Mars. My goal was to determine the thickness of water ice lost from the surface of Ceres over the course of the history of Ceres due to solar wind.

# **Modeling the Interior of Ceres**

Moment of Inertia

Moment of inertia is the rotational analog to mass; the distribution of mass within an object affects how that object will spin about a rotation axis. Two identical spheres will rotate about an axis the same way if an equal force is applied to them; however, if one of the spheres has its mass focused near the center while maintaining the same total mass and volume, it will require less force applied to it to rotate about the axis. Therefore, if an equal force is now applied to the two spheres, the one that with the mass focused near the center will rotate faster. The moment of inertia of an object can be related to the density and volume of the object, which can provide information about the radial distribution of mass within the interior. **Figure 2** shows the relationship between polar moment of inertia factor, C/M•a², and core size for Vesta (Zuber et al. 2011).

The moment of inertia for non-spherical planetary bodies is described with three parameters: A. B. and C. with C being the moment of inertia about the rotation axis. These values can be obtained by examining the mass distribution across the object. This change in mass distribution creates measurable differences in the gravity field of an object. Measurements in the gravity field can be used to make inferences about the difference in the moments of inertia C and A. The moment of inertia value, C, can be calculated from the moment of inertia difference, C-A, using two methods: observations of precession and assuming the body is hydrostatic. Precession is the change in the orientation of the rotation axis due to torque, with the rotation axis tracing a conical shape. The rate of precession increases with torque, which depends on C-A, and decreases with moment of inertia C; the rate of precession provides (C-A)/C. If the rate of precession and the object's gravitational field (giving us C-A) can be measured, then C can be found. If the rate of precession cannot be measured, C can also be derived directly from C-A assuming the object is hydrostatic. In this case, the expression for the flattening of a fluid body, which depends on C-A, can be compared to the Darwin-Radau approximation, which depends on C. (Bills and Nimmo 2011)

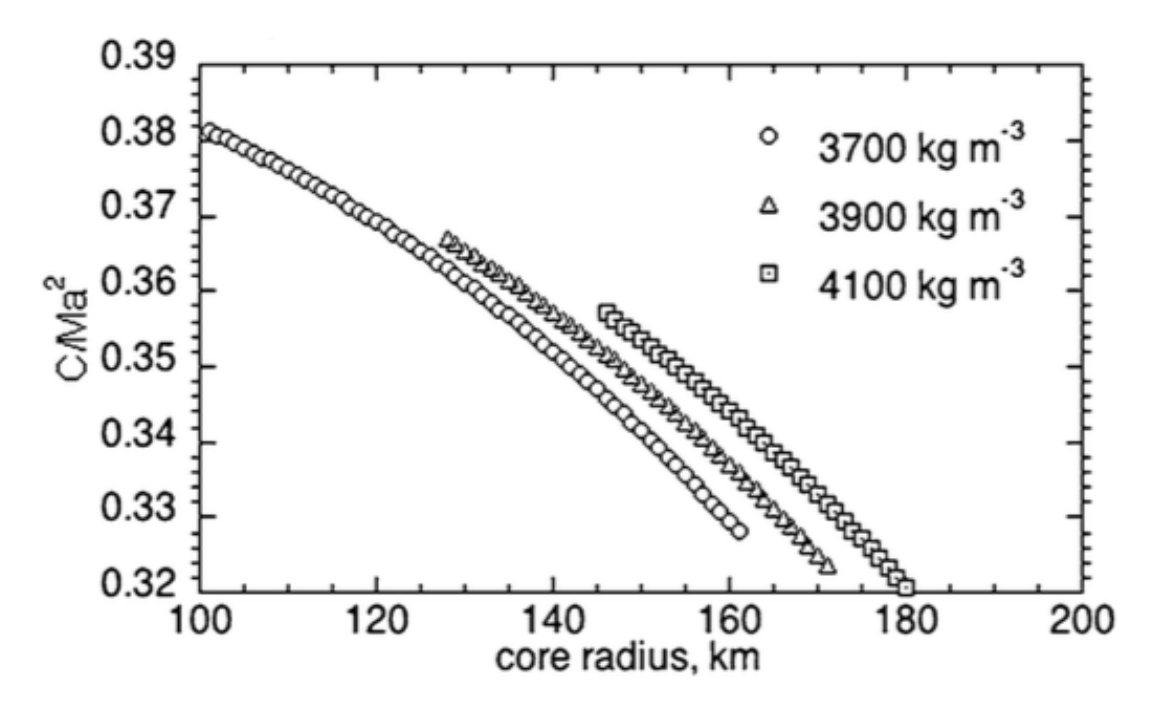


**Figure 2.** The plot Zuber et al. (2011) produced for a range of plausible bulk densities for ranges of polar moment of inertia and core radius. Calculation assumes a two-shell model of Vesta, core and mantle, with a mantle density of 2700 kg/m $^3$  and 3500 kg/m $^3$  and a core density of 7000 kg/m $^3$ . Moment of inertia as a function of core radius and bulk densities of the asteroid.

# Density Stratification in Ceres

This project used a two-shell spherical model for the density stratification Ceres. A spherical shape was used for simplicity and the near-spherical shape of Ceres. When creating the two-shell models the volume, mass, and mean density were used to solve for interior radius, interior density, and exterior density as a function of moment of inertia. The first three values are fixed values from the literature, which have been observed or calculated from previous missions, and the last three values are variable, given as a range of values, which are constrained by total radius and mean density (**Table 1**). I allow the interior radius to vary from zero to the radius of the asteroid (**Table 1**). The range of exterior densities is constrained by the observed composition of the surface and the mean density of the asteroid. The range of core densities is constrained by the previous values and the range of materials found in meteorites, planet interiors, and asteroid surface compositions. I calculated the resulting moment of inertia for each model, resulting in an n-model space, where n is the number of models, based on the range of values given for interior radius, interior density, and exterior density. This model space was then compared to the moments of inertia collected from the literature, to constrain the range of acceptable models of interior radius, interior density, and exterior density.

**Table 1.** Mass, radius, and moment of inertia values used for the density stratification model. Volume and mean density calculated from mass and radius. Density of compositional materials used as constraints.

	Value	Units	Reference	
Mass	9.4062 x 10 <sup>20</sup>	kg	Rambaux et al. 2015	
Radius	470.500	km	Rambaux et al. 2015	
Volume	4.363 x 10 <sup>17</sup>	m <sup>3</sup>	Calculated from Rambaux et al. 2015	
Mean Density	2.156 x 10 <sup>3</sup>	kg/m³	Calculated from Rambaux et al. 2015	
Moment of Inertia	0.36	N/A	Park et al. 2016	
Density of Rock	2930	kg/m³	Carmichael 1982	
Density of Water	1000	kg/m³	McCord and Sotin 2005	
Density of Phyllosilicate Clay	2800	kg/m³	Carmichael 1982	
Density of Iron	7900	kg/m³	McCord and Sotin 2005	

For any given value of exterior density, the acceptable interior radius and interior density can be calculated based on the relationships between the mass, density, and volume of an object and the total density, mass, and volume and the density, mass, and volume of parts of the object. The relationship between the mass, volume, and density of an object is

$$M_{Total} = V_{Total} \rho_{Total}$$
 Eq. 1

where  $M_{Total}$  is the total mass of the object in kilograms (kg),  $V_{Total}$  is the total volume of the object in meters cubed (m<sup>3</sup>), and  $\rho_{Total}$  is the total density of the object in kilograms per meters cubed (kg/m<sup>3</sup>). The relationship between total mass of an asteroid and the mass of the exterior and interior of the asteroid is

$$M_{Total} = M_{interior} + M_{exterior}$$
 Eq. 2

where  $M_{interior}$  is the mass of the interior of the object in kg, and  $M_{exterior}$  is the mass of the exterior of the object in kg. Likewise, the volume is:

$$V_{Total} = V_{interior} + V_{exterior}$$
 Eq. 3

where  $V_{interior}$  is the volume of the interior of the object in m<sup>3</sup>, and  $V_{exterior}$  is the volume of the exterior of the object in m<sup>3</sup>. The volume of a sphere relates to its radius:

$$V_{Total} = \frac{4}{3}\pi r_{Total}^{3}$$
 Eq. 4

where  $r_{Total}$  is the radius of the asteroid in m. The total mass can then be written as:

$$M_{Total} = \rho_{interior} V_{interior} + \rho_{exterior} V_{exterior}$$
 Eq. 5

Because the exterior radius is also unknown, the volume of the object and its interior is substituted:

$$M_{Total} = \rho_{interior} V_{interior} + \rho_{exterior} (V_{Total} - V_{interior})$$
 Eq. 6

$$M_{Total} = \rho_{interior} V_{interior} + \rho_{exterior} V_{Total} - \rho_{exterior} V_{interior}$$
 Eq. 7

The equation is rearranged to solve for interior density based on changes in interior radius,  $r_{interior}$ :

$$M_{Total} - \rho_{exterior} V_{Total} = V_{interior} (\rho_{interior} - \rho_{exterior})$$
 Eq. 8

$$\frac{M_{Total} - \rho_{exterior} V_{Total}}{V_{interior}} = \rho_{interior} - \rho_{exterior}$$
 Eq. 9

$$\frac{M_{Total} - \rho_{exterior} V_{Total}}{V_{interior}} + \rho_{exterior} = \rho_{interior}$$
 Eq. 10

$$\rho_{interior} = \frac{M_{Total} - \rho_{exterior} \frac{4}{3} \pi r_{Total}^{3}}{\frac{4}{3} \pi r_{interior}^{3}} + \rho_{exterior}$$
 Eq. 11

These equations were used in a MATLAB script to calculate the moment of inertia factor for changes in interior radius, interior density, and exterior density. The script assumes a spherical asteroid with two shells, labeled exterior and interior. It calculates the predicted moment of inertia for a range of interior radius and exterior density values that are bound by the following physical constraints. The range of the interior radius is bound by zero and the radius of the asteroid in meters. The range of the exterior density is bound by 1000 kg/m³, the density of water ice rounded to the nearest thousand, and the average density of the asteroid where the core is non-existent. The script bounds the range for interior density values between zero and the density of iron (**Table 1**). The results of this modeling are presented in **Figures 3** and **4**.

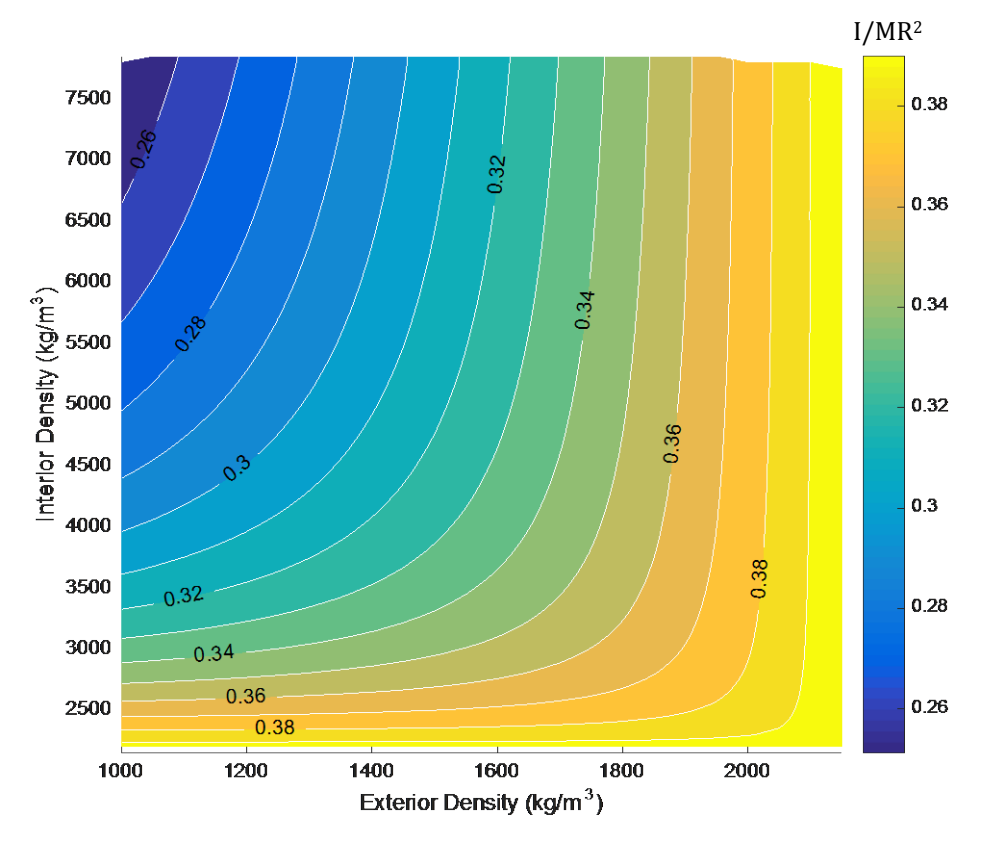


**Figure 3.** Parameters used to model Ceres using internal constraints from **Table 1**. This model plots the exterior density vs. interior density trade-off and displays their relationship with moment of inertia. Colorbar on the right shows the change in moment of inertia, with distinct values shown as lines on the plot.

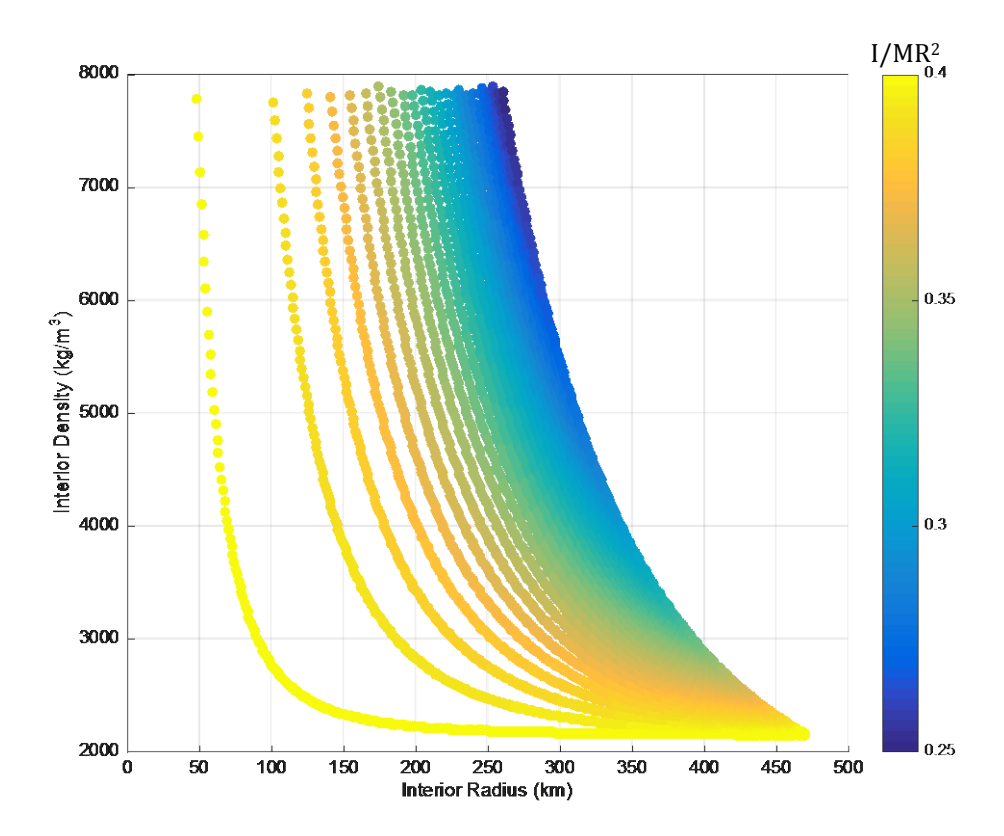


**Figure 4.** Relationship between interior density and interior radius, with associated moment of inertia for each set of values. Colorbar on the right shows the change in moment of inertia.

### Determining Exterior Composition of Ceres

**Figure 3** shows that there are a range of interior and exterior densities that satisfy the moment of inertia observation at Ceres. There is also a strong trade off between the density and size of the interior and density and thickness of the exterior. I used a three-phase mixing model to attempt to constrain the exterior composition for a given density to test the hypothesis that the exterior must contain significant volatiles, such as water ice, and examine the trade off between exterior density and assumed thickness and porosity. Factoring porosity into the three-phase mixing model allows the consideration of Zolotov's argument that an abrupt collapse in porosity can account for the stratified appearance (Zolotov 2009). One of the phases is porosity, and the remaining phases are calculated as percent of the remaining solid material. It allows the exterior density values from the density stratification model space to be given context, such as how much pore space is present and how much of the remaining material is clay or water ice.

The three-phase mixing model represents materials by their densities, but one phase of the mixing model is pore space in a vacuum, and uses a density of 0 kg/m $^3$ . I varied the following parameters: pore space is a assigned a value up to 50% and the remaining space is distributed between the other two phases, with one being assigned a value between 0% and 100%, and the other material provides the remaining percentage. **Figure 5** shows the resulting range of exterior compositions using ice, with a density of 1000 kg/m $^3$ , and phyllosilicates, with a density of 2800 kg/m $^3$ .

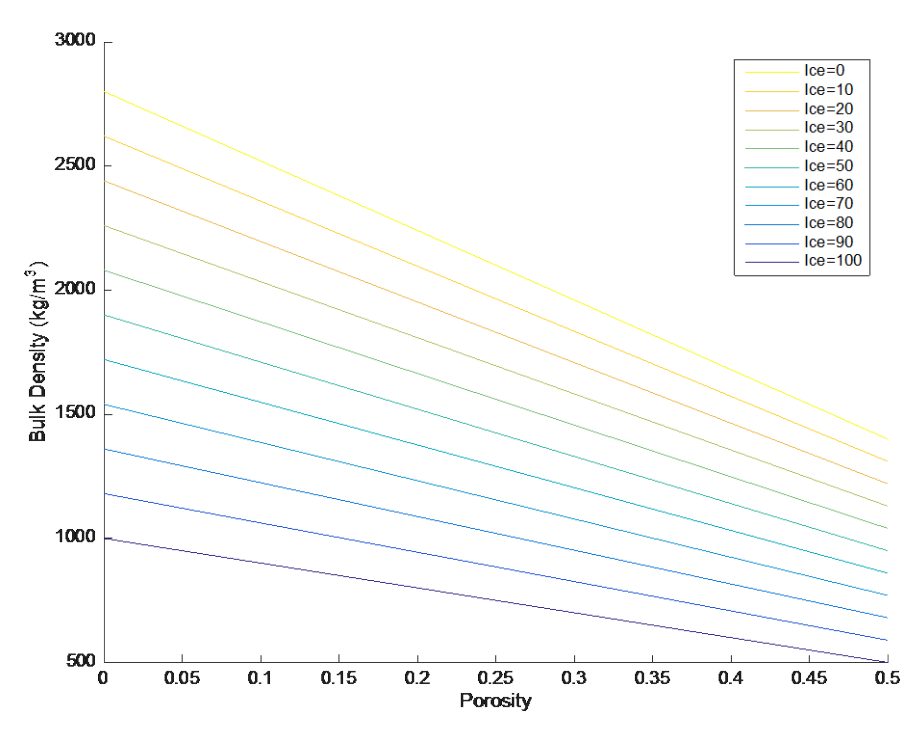


**Figure 5.** Relationship between bulk exterior density and the acceptable ice content, clay content, and porosity. The bulk exterior density ranges from  $1000 \text{ kg/m}^3$  to  $2800 \text{ kg/m}^3$  Colored lines represent % ice of non-porous material.

#### Discussion

A moment of inertia of 0.36 was used to constrain the values from **Figures 3 and 4**, calculated using the assumption of a hydrostatic Ceres (Park et al. 2016). There was not a formal estimate of uncertainties for the moment of inertia, so an error of 1%, similar to other moment of inertia estimates, is used during this discussion. This moment of inertia does not uniquely constrain the exterior density, interior density, or interior radius of Ceres. Figure 3 shows that an exterior density range from 1000 kg/m<sup>3</sup> to approximately 1900 kg/m<sup>3</sup> and an interior density range from approximately 2500 kg/m<sup>3</sup> to 7900 kg/m<sup>3</sup> is acceptable given the moment of inertia. This allows for two model spaces: a fixed, high-density exterior with a range of interior densities or a fixed, low-density interior with a range of exterior densities. The interior densities of the first space can be further divided into a highdensity interior, anything above silicate rocks, and a low-density interior, below silicate rocks. The exterior densities of the second space can be divided into a thick, low-density exterior dominated by water ice, and a thin, high-density exterior rich in clays. **Figure 4** illustrates that, given the acceptable interior density range of 2500 kg/m<sup>3</sup> and 7900 kg/m<sup>3</sup>, an interior radius between approximately 175 km and 450 km is acceptable with a 0.36 moment of inertia. The range of exterior densities from **figure 3** constrain the acceptable values for exterior composition in **figure 5**. Given the range of 1000 kg/m<sup>3</sup> to approximately 1900 kg/m<sup>3</sup>, the exterior composition is not highly constrained, with acceptable ice content ranging between approximately 95% and 0%.

The four ranges of model spaces from **figure 3** are not all equally likely, and some can be eliminated given current observations. There is a lack of water ice surface spectra, but the low density of Ceres suggests a high water ice content (McSween et al. 2016), so the lowest exterior densities can be ruled out, assuming the ice is mixed with volatiles or spread throughout Ceres. The apparent abundance of a clay-rich surface, with ammoniated phyllosilicates best fitting the average spectrum of Ceres (De Sanctis et al. 2016), point towards a higher exterior density. Although the density stratification model allows for a high density interior, current evidence supports a low density interior with a volatile-rich surface. Most thermal models for Ceres indicate a rocky core (McSween et al. 2016) and the presence of volatiles, such as ammonia and hydrogen rich regolith (McSween et al. 2016, Prettyman et al. 2016), support the exclusion of a higher density interior. These conclusions allow me to tentatively rule out the high density interior and low density exterior options, providing a new range of interior densities between approximately 2500 kg/m<sup>3</sup> and approximately 3500 kg/m<sup>3</sup> and exterior densities between approximately 1400 kg/m<sup>3</sup> and 1800 kg/m<sup>3</sup>.

Based on the assumption that an interior with a density higher than  $3500 \, \text{kg/m}^3$  can be ruled out, three models are presented as the differentiation and compositional models for Ceres. Two of the models represent the high and low extremes of the accepted densities for the interior and exterior, while the third is the median case. **Figure 6** represents a Ceres with the highest exterior and interior densities, as well as the smallest interior radius. From **figure 5**, the exterior density of  $1800 \, \text{kg/m}^3$  best matches a composition that has 20% pore space, with the

remaining material composed of 30% water ice and 70% clay. The interior density is slightly higher than the density of some basaltic rocks, such as norite, this may allow for the presence of excess metals (Carmichael 1982).

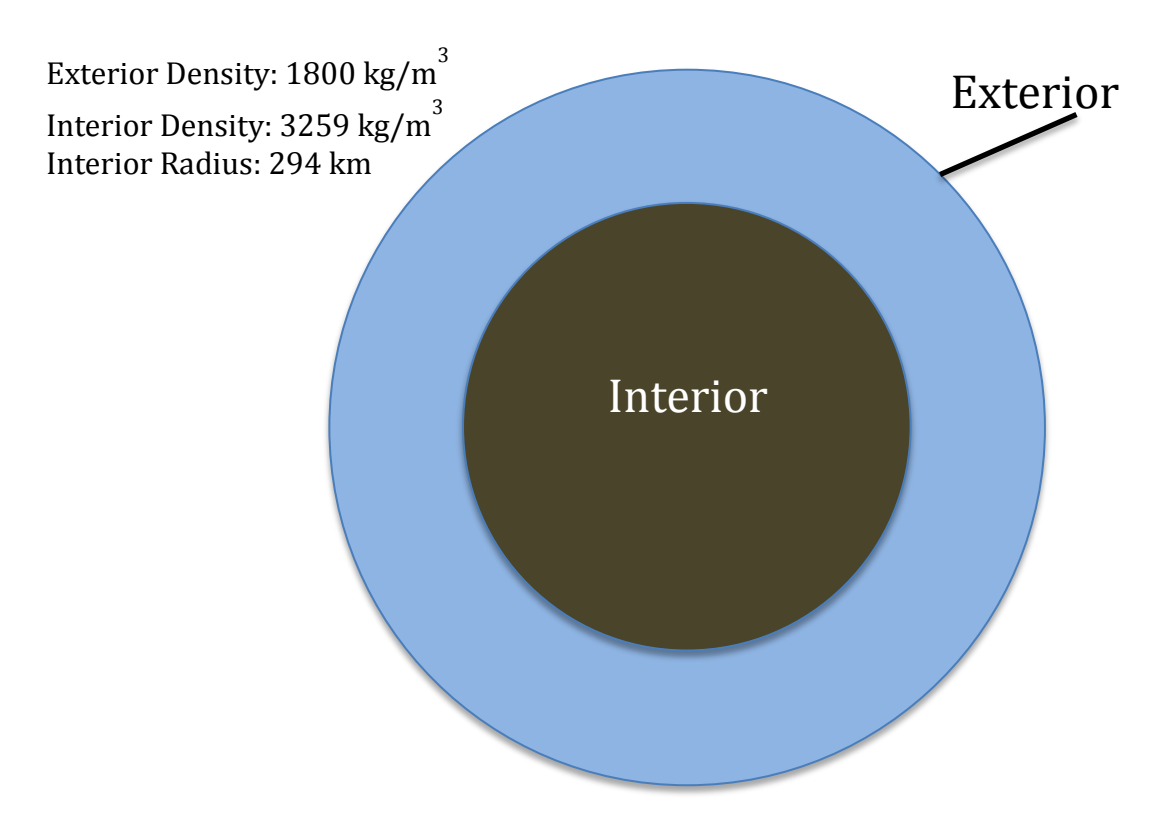


**Figure 6**. Model of Ceres with the densest interior and exterior that fits with the accepted moment of inertia of 0.36 (Park et al. 2016). From **figure 5**, the exterior of this model is clay rich.

**Figure 7** represents a Ceres the lowest exterior and interior densities, and the largest interior radius. From **figure 5** and **table 1**, the exterior density of 1000 kg/m<sup>3</sup> matches the density of water ice. The interior density is slightly less than the density of some felsic rocks, such as gneiss, which could indicate the presence of water (Carmichael 1982).

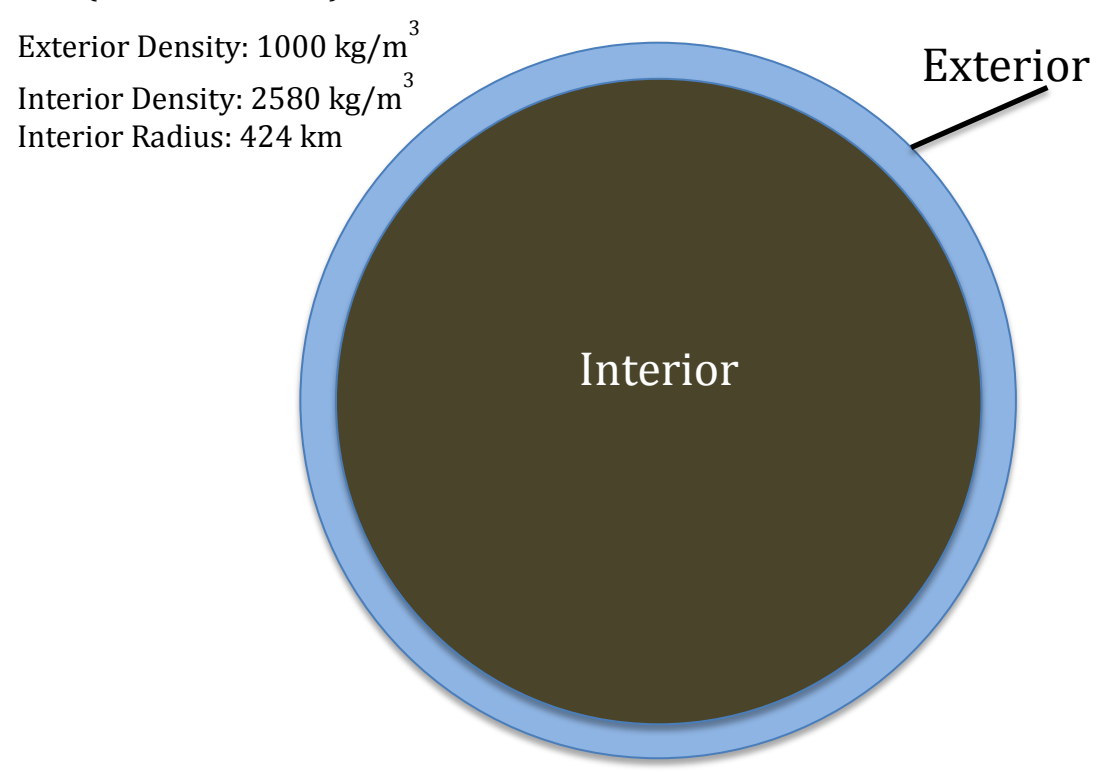


**Figure 7**. Model of Ceres with the least dense interior and exterior that fits within the accepted moment of inertia of 0.36 (Park et al. 2016). From **figure 5**, the exterior of this model is water ice.

**Figure 8** represents the median densities between **figures 6** and **7**. The exterior density of 1400 kg/m³ can be met with several compositional models. The simplest composition is 50% pore space and 50% clay. Another model has 20% pore space, with the remaining material composed of 60% water ice and 40% clay. The other close approximation to this exterior density has 30% pore space, with the remaining material composed of 40% water ice and 60% clay. The interior density is about the same as some felsic rocks, such as gneiss (Carmichael 1982).

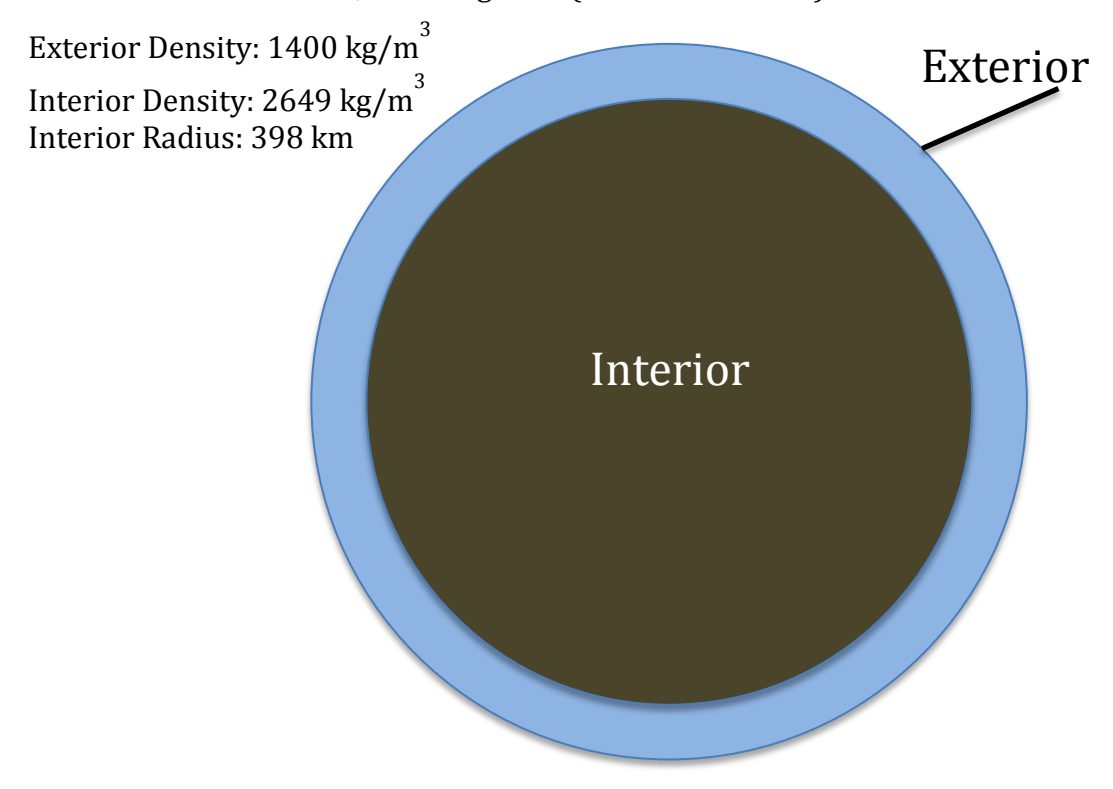


**Figure 8**. Intermediate model of Ceres that fits within the accepted moment of inertia of 0.36 (Park et al.). From **figure 5**, there are 3 possible compositions for the exterior; one composition is 50% pore space and 50% clay, the other two compositions are mixtures of pore space, water ice, and clay.

# **Presence of Liquid Water on the Surface of Ceres**

The clays on the surface of Ceres could suggest liquid water was present on Ceres at some point in its history, to allow for the in situ formation of the clay. Thermal evolution models from McCord and Sotin (2005) and Castillo-Rogez and McCord (2010) allow for the presence of liquid water in Ceres currently, but only in the interior. Castillo-Rogez and McCord (2010) produce models where an interior layer is warm enough to support liquid water during the evolution of Ceres, and based on other icy bodies is still likely in the present. The modeling done by McCord and Sotin (2005) result in water ice melting on Ceres, even when considering only long-lived radionuclide heating. This melt would become a liquid water mantle, and the circulating warm water would be able to alter surrounding rock (McCord and

Sotin, 2005). The clay on the surface of Ceres could have been formed at depth where liquid water was flowing earlier in the thermal history, but in situ formation of the clays would support the presence of liquid water on the surface of Ceres during its history.

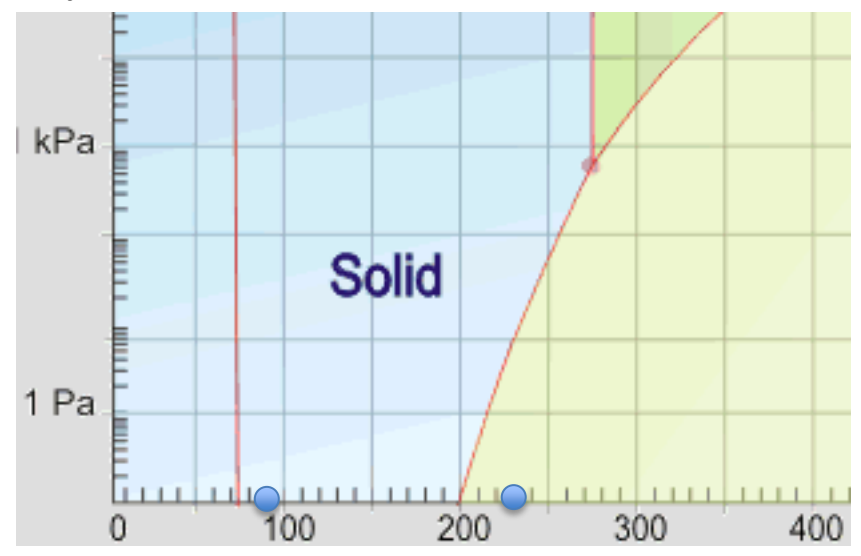


**Figure 9.** Phase diagram for  $H_2O$ , with temperature in Kelvin as x-axis and pressure in pascals as logarithmic y-axis. The blue shaded portion is the solid phase, the light green shaded portion is the vapor phase, and the green portion is the liquid phase. The blue points indicate the range of surface temperatures for Ceres from formation to present. Image adapted from: http://www1.lsbu.ac.uk/water/water\_phase\_diagram.html

Surface conditions on Ceres do not allow the presence of liquid water currently, with surface temperatures ranging from 90-150 K early in the thermal history of Ceres (Castillo-Rogez and McCord, 2010) and 231.5 K presently (McCord and Sotin, 2005), and a surface pressure of nearly zero, illustrated in **Figure 9.** The low temperature issue could be resolved due to the addition of salts reducing the melting point, which is suggested by McCord and Sotin (2005). In addition, if the pressure was increased for the current surface of Ceres, liquid water is possible. This pressure increase could be achieved if there was a layer of ice around Ceres that has since been removed. The minimum pressure required to begin supporting liquid water is 1 kPa and the surface gravity of Ceres is 0.285 m/s<sup>2</sup>, these values result in a minimum of 3.5 m, or 0.0035 km, of ice to present on top of the current surface of Ceres in order to support liquid water. The removal of this ice shell could have occurred through processes such as interaction with solar wind, thermal escape, or ejections of water vapor or water ice from impacts. This project focused on the interaction between solar wind and hydrogen ions and how much hydrogen could be lost in this fashion, and then using this hydrogen ion loss rate as an analog for H<sub>2</sub>O lost from the surface of Ceres over time.

There are no directly measured or calculated values for the rate of hydrogen ions loss from Ceres. The method that this project used to calculate a hydrogen ion loss rate for Ceres was to take reported values of hydrogen ion loss for Mars and Venus and use them as a reference. Venus and Mars were selected as planets of comparison due to their lack of strong magnetic fields, suggesting there is less shielding from solar wind. Hydrogen ion flux values from solar wind interaction

were collected from the literature for Venus and Mars, and were reported as both ions sec<sup>-1</sup> and ions sec<sup>-1</sup>cm<sup>-2</sup>. This project used the ions sec<sup>-1</sup> for calculations, so the values reported in ions sec<sup>-1</sup>cm<sup>-2</sup> had to be converted to ions sec<sup>-1</sup>, which was done by multiplying those values by the surface area of the body in question in cm<sup>2</sup>. The values for both Venus and Mars were averaged, and those average values were used to calculate the average hydrogen ion flux of a Ceres sized body at a range of distances from the Sun. To calculate the flux values for Ceres, a flux equation was derived, beginning with the proportional relationship between the flux and the inverse square of the distance as a ratio between the flux at Ceres and the flux at some other body, and then isolating the flux for Ceres:

$$\frac{f_{Ceres}}{f_1} = \frac{d_1^2}{d_2^2}$$
 Eq. 12

$$f_{Ceres} = f_1 \frac{d_1^2}{d_2^2}$$
 Eq. 13

where  $f_{Ceres}$  is the flux of Ceres,  $f_1$  is the flux of planet for comparison,  $d_1$  is the distance from the Sun to the planet for comparison, and  $d_2$  is a variable distance from the Sun.

The effect of the different sizes and surface gravity between Venus or Mars and Ceres also had to be taken into consideration, where the size of the body has a linear relationship with the flux and the surface gravity of the body has an inverse relationship with the flux:

$$\frac{f_{Ceres}}{f_1} = \frac{r_{Ceres}}{r_1}$$
 Eq. 14

$$\frac{f_{Ceres}}{f_1} = \frac{g_1}{g_{Ceres}}$$
 Eq. 15

where  $r_{Ceres}$  is the radius of Ceres,  $r_1$  is the radius of the planet for comparison,  $g_{Ceres}$  is the surface gravity of Ceres, and  $g_1$  is the surface gravity of the planet for comparison. Equations 13, 14, and 15 are combined, resulting in:

$$f_{Ceres} = f_1 \frac{d_1^2}{d_2^2} \frac{r_{Ceres}}{r_1} \frac{g_1}{g_{Ceres}}$$
 Eq. 16

The results of this comparison for flux for averaged literature values of Venus and Mars are in **Table 2**.

**Table 2.** Averaged Venus and Mars hydrogen ion loss rates from literature used to calculate the rate of hydrogen ion loss at Ceres due to solar wind. Sources for Venus and Mars average values from: Fox (1993), Lammer et al. (1996), Lammer et al. (2006), and Lammer et al. (2008)

	Rate used (H+/sec)	Ceres Upper Bound Rate (H+/sec)	Ceres Rate (H+/sec)	Ceres Lower Bound Rate (H+/sec)
Average Venus	$2.65 \times 10^{25}$	$1.73 \times 10^{25}$	$4.36 \times 10^{24}$	$1.10 \times 10^{24}$
Average Mars	$5.34 \times 10^{25}$	1.64 x 10 <sup>26</sup>	$2.92 \times 10^{25}$	$5.20 \times 10^{24}$

#### Discussion

With hydrogen ion loss serving as an analog for water loss, the values obtained from the previous calculation can be used to calculate the amount of water lost from the surface of Ceres during its history, which can then be used to calculate the thickness of an ice shell on top of Ceres. The first step is to convert the hydrogen ion flux into mass lost per second:

$$f_{Ceres} = \frac{H^+}{sec} * \frac{mole \ H^+}{6.022*10^{23} \ H^+} * \frac{mole \ H_2O}{2 \ moles \ H^+} * \frac{18.015 \ g \ H_2O}{mole \ H_2O} * \frac{1 \ kg}{1000 \ g} = \frac{kg \ H_2O}{sec}$$
Eq. 17

This converted rate of loss can then be used to calculate the mass lost throughout the history of Ceres. McCord and Sotin (2005) suggest that Ceres formed very early, probably within 10 million years of formation. For simplicity, I used an age of 4.6 billion year for the length of time Ceres has existed and experienced the effect of solar wind. This allows for the calculation of mass lost as:

$$\frac{kg H_2 O}{sec} * \frac{86400 sec}{day} * \frac{365 days}{year} * \frac{4.6*10^9}{1} = kg H_2 O lost$$
 Eq. 18

This mass of water lost is then converted into volume of water lost from the surface of Ceres by dividing this mass by the density of water, which can be seen in **Table 1**, and converting from m<sup>3</sup> to km<sup>3</sup>. With a volume of water lost, the thickness of an ice shell that was on the surface of Ceres can be calculated from:

$$V_{sphere} = \frac{4\pi}{3}r^3$$
 Eq. 19

where V is the volume of a sphere and r is the radius of the sphere.

In order to calculate the thickness of an ice shell on top of the present surface of Ceres, the r term must be arranged to account for the current radius of Ceres and the additional radius from the water ice:

$$V_{sphere} = \frac{4\pi}{3} ((r_{ice}^3 + r_{Ceres}^3) - r_{Ceres}^3)$$
 Eq. 20

this equation simplifies to a cubic function, which is then solved for  $r_{ice}$ . **Table 3** displays the results of the above method on the values obtained using the average Venus and Mars values (**Table 2**).

**Table 3.** The range of values for mass lost, volume lost, and the resulting thickness of a uniform ice shell around Ceres based on the Venus and Mars rates of loss.

	Upper	Ceres using	Lower Bound	Upper Bound	Ceres using	Lower Bound
	Bound using	Venus rate of	using Venus	using Mars	Mars rate of	using Mars
	Venus	loss			loss	
Mass Lost	$1.19 \times 10^{21}$	$6.41 \times 10^{20}$	$3.45 \times 10^{20}$	$3.21 \times 10^{17}$	$2.82 \times 10^{17}$	$2.48 \times 10^{17}$
(kg)						
Volume Lost	$1.19 \times 10^9$	6.41 x 10 <sup>8</sup>	$3.45 \times 10^{8}$	$3.21 \times 10^5$	$2.82 \times 10^{5}$	$2.48 \times 10^{5}$
(km <sup>3</sup> )						
Thickness of	20.2	5.1	1.3	192.1	34.2	6.1
Shell (m)						

Based on the averaged literature values for Venus and Mars, the thickness of an ice shell that could have been removed from the surface of Ceres could have been between 1.3 and 192.1 meters over the history of Ceres. Most of this range of ice shell loss raises the pressure enough to allow for liquid water on the present surface of Ceres, with only the range between the average Venus rate and the lower bound of the average Venus rate including an ice shell thickness too thin to raise the pressure enough for liquid water.

#### Conclusion

The internal structure and composition of Ceres is still uncertain. While multiple models have been proposed, a differentiated, two-shell model is one of the currently accepted interpretations. Using moment of inertia, I tested the hypothesis that Ceres is differentiated into an exterior and interior, and constrained the range of densities and interior radii that agree with the moment of inertia. I constrained the composition of the exterior using a three-phase mixing model. If the pressure on the present surface of Ceres was raised, liquid water may have been stable over the geologic history of Ceres. I also tested the hypothesis that liquid water could have existed on the present surface of Ceres by calculating the thickness of a uniform ice shell that could be removed due to interactions between solar wind and hydrogen ions, using Venus and Mars as a basis for calculating the rate of loss.

**Figures 6**, **7**, and **8** illustrate the range of differentiation and compositions for Ceres. Some conclusions can be drawn from these models, despite the moment of inertia not uniquely constraining the exterior density, interior density, or interior radius. **Figure 7** represents a Ceres with an exterior density of 1000 kg/m<sup>3</sup>, a value lower than was discussed as an acceptable exterior density. The **Figure 7** model could be eliminated if the composition of the exterior was entirely water ice. **Figures 6** and **8** appear to be more likely models. With three possible compositions for the exterior for the model in **figure 8**, there are multiple interpretations to explain this model. The 50% pore space and 50% clay composition could be interpreted as the result of impacts fracturing the exterior, but does not explain the presence of the clay without alteration from water. The other two compositions incorporate pore space, water ice, and clay. These compositions represent a more likely exterior composition, with the water ice content allowing the alteration required for the clay. The interior radius of the **figure 6** model is similar to the core radius estimate by Park et al. (2016) and displays the greatest differentiation of the three models. Of the three models produced, the highest density interior and exterior model (**figure 6**) appears to be the best fit, based on the degree of differentiation and the composition of the exterior.

This project only focused on the interaction between solar wind and hydrogen ions and the potential comparison that can be drawn from Venus and Mars to Ceres. Although the majority of solar wind interaction rates allow for a uniform ice shell thickness that raises the pressure enough for liquid water, thermal loss has not been factored in at this time. The qualitative effect of ejection of material from impacts has not been thoroughly investigated for this project.

Different crater counting methods indicate a number of large craters on Ceres that are not seen, and though some relics of impact craters have been potentially identified, there is still a missing number (Marchi et al. 2016). Marchi et al. (2016) also suggests that relaxation doesn't explain this lack of craters, and while they suggest that these missing craters could be interpreted as Ceres having migrated inward, it could also indicate an ice shell that is no longer present (Castillo-Rogez, 2016).

This method produces possible rates of hydrogen ion loss from Ceres due to solar wind, but these rates are limited by the starting assumptions that produced the hydrogen ion loss values I obtained from the literature. These calculated rates for Ceres serve as potential bounds for the hydrogen ion loss due to solar wind. The ice shell thickness calculated from these rates is also an upper bound, because it assumes that the maximum amount of water that can be lost was present. There are other differences between Venus and Mars and Ceres that could affect these results, such as Ceres likely not ever having any sort of magnetic field, where Venus and Mars either have weak magnetic fields or had stronger magnetic fields in the past. These results assume the rate of loss of hydrogen ions has been constant throughout time, and a change in the rate would also affect the results of this project. The range of ice shell thickness from **Table 3** indicate that solar wind could account for most of the ice shell loss required to raise the pressure enough to support liquid water, and thermal escape may be able to account for the rest.

Based on the results of the interior modeling of Ceres, the hypothesis that Ceres is differentiated is supported. The results of the three-phase mixing model supports the hypothesis that the interior and exterior of Ceres have distinct compositions. The results of the hydrogen ion loss rate from Ceres supports the hypothesis that liquid water could have been present on the surface of Ceres in its geologic history. Although the hypotheses of this project have been supported, future work could be done to further constrain or enhance the results. The interior modeling could be modified to allow for a better representation of the shape of Ceres as well as multiple interior layers. The thickness of a potential ice shell around Ceres could be improved with further study of the influence of solar wind with Ceres, as well as other sources of water loss, such as thermal loss or the ejection of water from the interior of Ceres due to cryovolcanism.

#### **References Cited**

- Asteroids. Retrieved November 21, 2015, from http://nssdc.gsfc.nasa.gov/planetary/planets/asteroidpage.html
- Bills, B. and Nimmo, F., 2011. Forced obliquities and moments of inertia of Ceres and Vesta. *Icarus* 213, 496-509.
- Carmichael, R. S. (1982). *Handbook of Physical Properties of Rocks* (Vol. 2). Boca Raton, FL: CRC Press.
- Castillo-Rogez, J.C., Bowling, T., Fu, R.R.CR., McSween, H.Y., Raymond, C.A., Rambaux, N., Travis, B., Marchi, S., O'Brien, D.P., Johnson, B.C., King, S.D., Bland, M.T., Neveu, M., De Sanctis, M.C., Ruesch, O., Sykes, M.V., Prettyman, T.H., Park, R.S., Russel, C.T., 2016. Loss of Ceres' icy shell from impacts: Assessment and implications. *Lunar and Planetary Science Conference 47*, 3012.
- Castillo-Rogez, J.C. and McCord, T.B., 2010. Ceres' evolution and present state constrained by shape data. *Icarus* 205, 443-459.
- Chassefiere, E., 1996. Hydrodynamic escape of hydrogen from a hot water-rich atmosphere: The case of Venus. *Journal of Geophysical Research 101*, 26039-26056.
- Chalov, S., 2006. Interstellar Pickup Ions and Injection Problem for Anomalous Cosmic Rays: Theoretical Aspect. *The Physics of the Heliospheric Boundaries*.
- De Sanctis, M.C., Ammannito, E., Carrozzo, F.G., Ciarniello, M., Frigeri, A., Longobardo, A., Palomba, E., Raponi, A., Tosi, F., Zambon, F., Fonte, S., Formisano, M., Giardino, M., Magni, G., Capaccioni, F., Capria, M.T., Marchi, S., Pieters, C.M., Ehlmann, B.L., McCord, T.B., Combe, J.-Ph., McSween, H.Y., Jaumann, R., McFadden, L.A., Joy, S., Polanskey, C.A., Rayman, M.D., Raymond, C.A., Russel, C.T., and the Dawn Science Team (2016). Ceres Composition By VIR On Dawn: Highlights of the First Year of Observation. *Lunar and Planetary Science Conference 47*, 1832.
- Fox, J.L., 1993. On the escape of oxygen and hydrogen from Mars. *Geophysical Research Letters 20*, 1847-1850.
- Konopliv, A.S., Asmar, S.W., Bills, B.G., Mastrodemos, N., Park, R.S., Raymond, C.A., Smith, D.E., Zuber, M.T., 2011. The Dawn Gravity Investigation at Vesta and Ceres. *Space Sci. Rev.* 163, 461-486.
- Kulikov, Y.N., Lammer, H., Lichtenegger, H.I.M., Terada, N., Ribas, I., Kolb, C., Langmayr, D., Lundin, R., Guinan, E.F., Barabash, S., and Biernat, H.K., 2006. Atmospheric and water loss from early Venus. *Planetary and Space Science* 54, 1425-1444.
- Lammer, H., Kasting, J.F., Chassefiere, E., Johnson, R.E., Kulikov, Y.N., Tian, F., 2008. Atmospheric escape and evolution of terrestrial planets and satellites. *Space Science Review 139*, 399-436.
- Lammer, H., Lichteneggar, H.I.M., Biernat, H.K., Erkav, N.V., Arshukova, I.L., Kolb, C., Gunell, H., Lukyanov, A., Holmstrom, M., Barabash, S., Zhang, T.L., and Baumjohann, W., 2006. Loss of hydrogen and oxygen from the upper atmosphere of Venus. *Planetary and Space Science* 54, 1445-1456.
- Lammer, H., Lichteneggar, H.I.M., Kolb, C., Ribas, I., Guinan, E.F., Abart, R., Bauer, S.J., 2003. Loss of water from Mars: Implications for the oxidation of the soil. *Icarus* 165, 9-25.
- Lammer, H., Stumptner, W., and Bauer, S.J., 1996. Loss of H and O from Mars: Implications for the planetary water inventory. *Geophysical Research Letters* 23, 3353-3356.
- Marchi, S., Ermakov, A.I., Raymond, C.A., Fu, R.R., O'Brien, D.P., Bland, M.T., Ammannito, E., De Sanctis, M.C., Bowling, T., Schenk, P., Scully, J.E.C., Buczkowski, D.L., Williams, D.A., Hiesinger, H., and Russel, C.T., 2016. The missing large impact craters on Ceres. *Nature Communications*, 1-9.

- McCord, T.B., and Sotin, C., 2005. Ceres: Evolution and current state. *Journal of Geophysical Research* 110, 1-14.
- McSween, H.Y., Castillo-Rogez, J., Emery, J.P., De Sanctis, M.C., and the Dawn Science Team, 2016. Rationalizing the composition and alteration of Ceres. *Lunar and Planetary Science Conference* 47, 1258.
- Millis, R.L. Wasserman, L.H., Franz, O.G., Nye, R.A., Oliver, R.C., Kreidl, T.J., Jones, S.E., Hubbard, W., Lebofsky, L., Goff, R., Marcialis, R., Sykes, M., Frecker, J., Hunten, D., Zellner, B., Reitsema, H., Schneider, G., Dunham, E., Klavetter, J., Meech, K., Oswalt, T., Rafert, J., Strother, E., Smith, J., Povenmire, H., Jones, B., Kornbluh, D., Reed, L., Izor, K., A'Hearn, M.F., Schnurr, R., Osborn, W., Parker, D., Douglas, W.T., Beish, J.D., Klemola, A.R., Rios, M., Sanchez, A., Piironen, J., Mooney, M., Ireland, R.S., and Leibow, D., 1987. The Size, Shape, Density, and Albedo of Ceres from Its Occultation of BD+8°471. *Icarus* 72, 507-518.
- Nelson, M.L., Britt, D.T., Lebofsky, L.A., 1993. Review of Asteroid Compositions. *Resources of Near-Earth Space*, 493-522.
- Neveu, M., and Desch, S.J., 2016. Geochemistry, thermal evolution, and cryovolcanism on Ceres with a muddy ice mantle. *Lunar and Planetary Science Conference* 47, 1384.
- Park, R.S., Konopliv, A.S., Bills, B., Castillo-Rogez, J., Asmar, S.W., Rambaux, N., Raymond, C.A., Russel, C.T., Zuber, M.T., Ermakov, A., King, S.D., and Rayman, M.D., 2016. Gravity science investigation of Ceres from Dawn. *Lunar and Planetary Science Conference* 47. 1781.
- Prettyman, T.H., Yamashita, N., Castillo-Rogez, J.C., Feldman, W.C., Lawrence, D.J., McSween, H.Y., Schorghofer, N., Toplis, M.J., Forni, O., Joy, S.P., Marchi, S., Platz, T., Polanskey, C.A., de Sanctis, M.C., Rayman, M.D., Raymond, C.A., and Russel, C.T., 2016. Elemental composition of Ceres by Dawn's gamma ray and neutron detector. *Lunar and Planetary Science Conference* 47, 2228.
- Rambaux, N., Chambat, F., and Castillo-Rogez, J.C., 2015. Third-order development of shape, gravity, andmoment of inertia for highly flattened celestial bodies. Application to Ceres. *Astronomy and Astrophysics* 584, 1-8.
- Rivkin, A.S., Volquardsen, E.L., and Clark, B.E., 2006. The surface composition of Ceres: Discovery of carbonates and iron-rich clays. *Icarus* 185, 563-567.
- Williams, R. Mars Fact Sheet. Retrieved October 29, 2016, from http://nssdc.gsfc.nasa.gov/planetary/factsheet/marsfact.html
- Williams, R. Venus Fact Sheet. Retrieved October 29, 2016, from http://nssdc.gsfc.nasa.gov/planetary/factsheet/venusfact.html
- Zolotov, M.Y., 2009. On the composition and differentiation of Ceres. *Icarus 204*, 183-193.
- Zuber, M.T., McSween, H.Y., Binzel, R.P., Elkins-Tanton, L.T., Konopliv, A.S., Pieters, C.M., Smith, D.E., 2011. Origin, Internal Structure and Evolution of 4 Vesta. *Space Sci. Rev.* 163, 77-93.

Honor Code

I pledge on my honor that I have not given or received any unauthorized assistance or plagiarized on this assignment.

Joshua McAinsh Gaal